

1
2
3
4
5
6
7
8
9
10
11
12
13
14
15
16
17
18
19
20
21
22
23
24
25
26
27
28
29
30
31
32
33

Cell-free glycoengineering of the recombinant SARS-CoV-2 spike glycoprotein

Johannes Ruhnau ^{1†}, Valerian Grote ^{1†}, Mariana Juarez-Osorio ¹, Dunja Bruder ^{2,3}, Erdmann Rapp ^{1,4}, Thomas F. T. Rexer ^{1*}, Udo Reichl ^{1,5}

[†] These Authors share first authorship

¹ Max Planck Institute for Dynamics of Complex Technical Systems, Bioprocess Engineering, Sandtorstr. 1, 39106 Magdeburg, Germany

² Infection Immunology Group, Institute of Medical Microbiology, Infection Prevention and Control, Health Campus Immunology, Infectiology and Inflammation, Otto-von-Guericke University Magdeburg, Germany

³ Immune Regulation Group, Helmholtz Centre for Infection Research, Braunschweig, Germany

⁴ glyXera GmbH, Brenneckestr. 20 - ZENIT, 39120 Magdeburg, Germany

⁵ Otto-von-Guericke University Magdeburg, Chair of Bioprocess Engineering, Magdeburg, Germany

*** Correspondence:**

Thomas Rexer
rexer@mpi-magdeburg.mpg.de

Keywords: SARS-CoV-2, COVID-19, glycoengineering, cell-free synthetic biology, subunit vaccine

34 **Abstract**

35 The baculovirus-insect cell expression system is readily utilized to produce viral glycoproteins for
36 research as well as for subunit vaccines and vaccine candidates, for instance against SARS-CoV-2
37 infections. However, the glycoforms of recombinant proteins derived from this expression system
38 are inherently different from mammalian cell-derived glycoforms with mainly complex-type *N*-
39 glycans attached, and the impact of these differences in protein glycosylation on the
40 immunogenicity is severely underinvestigated. This applies also to the SARS-CoV-2 spike
41 glycoprotein, which is the antigen target of all licensed vaccines and vaccine candidates including
42 virus like particles and subunit vaccines that are variants of the spike protein. Here, we expressed
43 the transmembrane-deleted human β -1,2 N-acetylglucosamintransferases I and II (MGAT1 Δ TM
44 and MGAT2 Δ TM) and the β -1,4-galactosyltransferase (GalT Δ TM) in *E. coli* to *in-vitro* remodel
45 the *N*-glycans of a recombinant SARS-CoV-2 spike glycoprotein derived from insect cells. In a
46 cell-free sequential one-pot reaction, fucosylated and afucosylated paucimannose-type *N*-glycans
47 were converted to complex-type galactosylated *N*-glycans. In the future, this *in-vitro*
48 glycoengineering approach can be used to efficiently generate a wide range of *N*-glycans on
49 antigens considered as vaccine candidates for animal trials and preclinical testing to better
50 characterize the impact of *N*-glycosylation on immunity and to improve the efficacy of protein
51 subunit vaccines.

52

53

54 1 Introduction

55 Most epidemics caused by viral infections that are associated with a significant death toll were
56 caused by enveloped viruses such as influenza A virus, human immunodeficiency virus (HIV),
57 Zika virus, Yellow fever virus, Dengue virus and Ebolavirus. Often, the main target for
58 neutralizing antibodies to evoke a strong immune response is a glycosylated envelope
59 membrane protein. Thus, in the development of vaccines, glycoproteins are typically in the
60 focus of interest. In general, the glycosylation of proteins plays a critical role regarding structure,
61 function, solubility, stability, trafficking, and ligand-binding (Imperiali and O'Connor,
62 1999; Dalziel et al., 2014; Varki, 2017). Furthermore, glycosylation plays a major role for
63 pharmacokinetics and pharmacodynamics of biologics and for pathogen-host interaction
64 (Bagdonaite and Wandall, 2018; Cymer et al., 2018; Watanabe et al., 2019). In viral
65 pathogenesis, glycosylation affects the attachment and release of virus particles as well as
66 immune evasion (Schön et al.; Bagdonaite and Wandall, 2018; Watanabe et al., 2019).
67 Especially the latter is a major hurdle for vaccine design. The mode of actions that are known
68 to be employed to invade the immune system are secretion and shedding of glycoproteins that
69 function as a decoy to the immune system, and the shielding of epitopes (Watanabe et al., 2019).
70 The latter is facilitated by occluding antigenic epitopes with host-derived glycans that are
71 obtained through hijacking the host's cellular glycosylation machinery (Pralow et al.; Schwarzer
72 et al., 2009; Francica et al., 2010; Helle et al., 2011; Rödig et al., 2011; Rödig et al.,
73 2013; Sommerstein et al., 2015; Behrens et al., 2016; Gram et al., 2016; Walls et al., 2016).
74 Moreover, it has been shown that also the glycoform itself can have an impact on binding and
75 transmission assay as well as on transmissibility, antigenicity, and immunogenicity in animal
76 models (Lin et al., 2003; Hütter et al., 2013; Chen et al., 2014; Li et al., 2016; Go et al., 2017).
77 While it is assumed that immunogenic antigens benefit from mimicking the glycosylation of
78 host cell proteins, it has also been proposed that modification of specific terminal sugar residues
79 could be used to amplify vaccine efficacy (Galili, 2020; Chen, 2021). However, due to the
80 complexity of protein glycosylation and the prevailing lack of methods to introduce defined
81 modifications in the glycan composition of the proteins of interest, the topic is
82 underinvestigated (Schön et al.; Watanabe et al., 2019; Grant et al., 2020).

83 The ongoing corona virus disease 2019 (COVID-19) pandemic is caused by the severe acute
84 respiratory syndrome coronavirus 2 (SARS-CoV-2) – a single-stranded, positive-sense RNA
85 virus (Walls et al., 2020). Its membrane envelope consists of three membrane proteins: the
86 surface spike (S) glycoprotein, an integral membrane protein and an envelope protein (Wan et
87 al., 2020; Zhou et al., 2020). Virus entry into human host cells is mediated by the S glycoprotein
88 that binds to angiotensin-converting enzyme 2 (Walls et al., 2020). The S protein has 22
89 N-linked glycosylation sites. Thus, it is significantly more glycosylated than, for instance, the
90 influenza A hemagglutinin (Wrapp et al., 2020). For the SARS-CoV-1 spike protein it has been
91 shown previously that *N*-glycans significantly impact antibody response and neutralizing
92 antibody levels (Chen et al., 2014; Walls et al., 2020).

93 For the investigation of the impact of glycoforms on the immunogenicity, mainly animal cell
94 lines such as HEK and CHO cells that produce differentially glycosylated proteins are
95 employed (Schön et al.; Lin et al., 2013). However, due to need to develop specific expression
96 protocols for each cell line, this approach is highly work-intensive. Additionally, the inherent
97 macro- and microheterogeneity of glycoproteins complicate the elucidation of the role of
98 specific glycans in, for instance, regarding their immunogenicity in animal models.

99 Over the past years the establishment of protocols for expression of eukaryotic and bacterial
100 glycosyltransferases has facilitated the processing of glycans in cell-free one-pot reactions. As
101 a platform technology, the corresponding *in-vitro* glycoengineering approaches have the
102 potential to tailor the glycoform of proteins independent of the expression systems used (Van

103 Landuyt et al., 2019;Rexer et al., 2020a). In our study, recombinant human β -1,2 N-
104 acetylglucosamintransferases I and II (MGAT1 Δ TM and MGAT2 Δ TM) and the β -1,4-
105 galactosyltransferase (GalT Δ TM) expressed in *E. coli* were utilized to convert insect cell-
106 derived paucimannose structures of recombinant SARS-CoV-2 spike glycoprotein to typical
107 mammalian, complex-type galactosylated structures in a cell-free one-pot reaction (Fujiyama
108 et al., 2001;Boeggeman et al., 2003;Bendiak, 2014;Ramakrishnan and Qasba, 2014;Stanley,
109 2014). Glycan structures were analyzed using multiplexed capillary gel electrophoresis with
110 laser-induced fluorescence detection (xCGE-LIF) and Matrix-assisted laser
111 desorption/ionization time-of-flight mass spectrometry (MALDI-TOF-MS). Results obtained
112 clearly demonstrate that a large fraction of fucosylated and afucosylated, Man3-glycans were
113 transferred to biantennary G2 and G2F structures (also see Table 1).

114

115

116 **2 Materials and Methods**

117 **2.1 Enzymes**

118 SARS-CoV-2 spike protein containing the S1 subunit and the S2 subunit ectodomain was
119 purchased from SinoBiologica (Beijing, PR China). The recombinant protein was produced
120 using the baculovirus-insect-cell expression system using High-Five™ cells. The protein bears
121 a C-terminal His-tag. For all other materials see supporting information (SI).

122 2.1.1 Gene expression - Genes encoding for the transmembrane deleted (Δ TM) variants of
123 *Homo sapiens* α -1,3-mannosyl-glycoprotein 2- β -N-acetylglucosaminyltransferase
124 (MGAT1 Δ TM) (E.C. 2.4.1.201), α -1,6-mannosyl-glycoprotein 2- β -N-
125 acetylglucosaminyltransferase (MGAT2 Δ TM) (E.C. 2.4.1.143) and β -N-
126 acetylglucosaminylglycopeptide β -1,4-galactosyltransferase (GalT Δ TM) (E.C. 2.4.1.38) were
127 expressed in *E. coli*. All constructs are bearing a 6 x histidine-tag (His-tag). For information on
128 the cultivation, strains and vectors used see SI.

129 2.1.2. Purification by ion metal affinity chromatography - *E. coli* cells were lysed at 4°C by
130 high-pressure cell disruption (3 cycles, 400-600 bar) using an HPL6 homogenizer (Maximator
131 GmbH, Nordhausen, Germany) followed by centrifugation at 7200 x g for 20 min at 4°C to
132 precipitate cell debris. The overexpressed enzymes were filtered through 8 μ m syringe filters
133 and then purified by ion metal chromatography using an ÄKTA™ start system equipped with
134 HisTrap™ HP columns (1 mL) (both GE Healthcare Life Sciences, Little Chalfont, UK). A
135 buffer exchange was carried out to remove excess imidazole using an Amicon® Ultra-15
136 Centrifugal Filter Unit – 3 kDa MW cutoff (UFC900308, Darmstadt, Germany) using standard
137 procedures. Enzymes were stored in 50% (v/v) glycerol stock solutions at -20°C. Enzyme
138 concentrations were determined by performing a bicinchoninic acid (BCA) assay using the
139 Pierce™ BCA Protein Assay Kit (Thermo Fisher Scientific; Waltham, USA).

140

141 **2.2 One-pot *in-vitro* glycoengineering reactions**

142 Reactions were performed by sequential addition of enzymes in buffered (25 mM HEPES, pH
143 6.5) aqueous solutions supplemented with 10 mM MnCl₂ at 37°C under shaking (550 rpm). The
144 initial reaction volume (1 mL) contained 0.1 μ g/mL of SARS-CoV-2 spike protein, 4 mM UDP-
145 GlcNAc and 0.2 μ g/ μ L MGAT1 Δ TM. After a reaction time of 12 h, 150 μ L of a buffered
146 solution containing 4 mM UDP-GlcNAc and 0.85 μ g/ μ L MGAT2 Δ TM was added to 500 μ L
147 of the reaction. After 12 more hours, 175 μ L of a buffered solution containing 4 mM UDP-

148 galactose and 0.56 $\mu\text{g}/\mu\text{L}$ GalT Δ TM was added to 325 μL of the reaction mix. Aliquots of the
149 reactions were taken for *N*-glycan analysis before the addition of each enzyme and at the end
150 of the reaction (12 h after GalT Δ TM addition).

151 2.2.1 Sample pretreatment: PNGase F digest of *N*-glycosylated proteins - 1 μg *N*-glycosylated
152 protein sample was linearized and denatured by adding 2 μL 2 % (w/v) SDS in PBS buffer (pH
153 7.2) and subsequent heating at 60°C for 10 min. Samples were cooled down to room
154 temperature. 4 μL 8 % (w/v) IGEPAL in PBS and 1 μL of a 1 U/ μL PNGase F solution were
155 added. Samples were incubated for 1 h at 37°C, vacuum evaporated and dissolved in 20 μL LC-
156 MS grade H₂O.

157 2.2.2 xCGE-LIF-based *N*-Glycan Analysis - *N*-glycan analysis based on xCGE-LIF was
158 conducted using a glyXboxCETM-system (glyXera, Magdeburg, Germany) according to
159 (Hennig et al., 2015; Hennig et al., 2016). Briefly, 2 μL of each sample was used for fluorescent
160 labelling of *N*-glycans with 8-aminopyrene-1,3,6-trisulfonic acid (APTS) following post
161 derivatization clean-up by hydrophilic interaction liquid chromatography-solid phase extraction
162 (HILIC-SPE) with the glyXprep16TM kit (glyXera). Data processing, normalization of
163 migration times and annotation of *N*-glycan fingerprints were performed with glyXtoolTM
164 software (glyXera).

165 2.2.3. MALDI-TOF-MS-based *N*-Glycan Analysis - MALDI-TOF-MS analysis of released *N*-
166 glycans was performed as described previously (Selman et al., 2011; Fischöder et al., 2019).
167 Briefly, 0.9 cm cotton rope was used for Cotton HILIC SPE. The stationary phase was
168 equilibrated with 50 μL LC-MS grade H₂O followed by 50 μL 85% ACN_{aq}. 10 μL of released
169 *N*-glycans were adjusted to 70 μL 85% ACN_{aq} with 1% TFA and loaded onto the HILIC phase.
170 Following 2 washing steps with 50 μL 85% ACN_{aq} with 1% TFA and 50 μL 85% ACN_{aq}, the
171 samples were eluted in 70 μL LC-MS grade H₂O, vacuum evaporated and dissolved in 20 μL
172 LC-MS grade H₂O. For the MALDI-TOF-MS analysis 0.5 μL super-dihydroxybenzoic acid (S-
173 DHB) ($\geq 99.0\%$, Sigma-Aldrich, Steinheim, Germany) matrix (10 mg/mL) in 30% (v/v) ACN_{aq},
174 0.1% (v/v) TFA, 2 mM NaCl was spotted onto a MTP AnchorChip 800/384 TF MALDI target
175 (Bruker Daltonics, Bremen, Germany). Subsequently 1 μL sample was applied onto the dried
176 matrix layer. Measurements were carried out on an ultrafleXtreme MALDI-TOF/TOF MS
177 (Bruker Daltonics, Bremen, Germany) in reflectron positive ion mode. Data was processed with
178 the top-hat filter and the adjacent-averaging algorithm using flexAnalysis version 3.3 Build 80
179 (Bruker Daltonics, Bremen, Germany).

180

181 **2.3 *N*-Glycan Nomenclature**

182 *N*-Glycan nomenclature was adopted from Stanley et al (Stanley et al., 2015). Depiction of *N*-
183 glycan structures followed the Symbol Nomenclature for Glycans (SNFG) guidelines
184 (Neelamegham et al., 2019). The *N*-glycan sketches in this manuscript were produced using the
185 “Glycan Builder2” software tool (Tsuchiya et al., 2017). *N*-Glycans are typically categorized
186 into paucimannose-, oligomannose-, hybrid- and complex-type structures.

187

188 **3 Results**

189 **3.1 Pathway design**

190 The human *in-vivo* cascade reaction for the generation of complex-type *N*-glycans from the
191 conserved ER-derived oligomannose-type *N*-glycan precursor GlcNAc₂Man₉Glc₃, was in part
192 remodelled *in-vitro* to generate fully galactosylated complex-type *N*-glycans starting from
193 insect cell-derived paucimannose-type *N*-glycans. Central to the construction of the simplified
194 *in-vitro* cascade is the ability of human MGAT1 to utilize Man3 and Man3F as substrates, which
195 allows circumventing the application of recombinant mannosidases (see Figure 1). For the
196 production of the G2 structure from paucimannose-type *N*-glycans, the three recombinant
197 glycosyltransferases MGAT1 Δ TM, MGAT2 Δ TM and GalT Δ TM were successfully produced
198 in *E. coli* (see SI). Enzyme concentrations of typically 1.3 mg/mL after ion metal affinity
199 chromatography (IMAC) and buffer exchange were obtained. In scouting experiments, it was
200 confirmed that all enzymes are active in the buffered solutions (pH 6.5) with MnCl₂
201 supplemented as a co-factor (data not shown).

202

203 **3.2 Glycoform of the unprocessed recombinant SARS-CoV-2 spike glycoprotein**

204 Analytical characterization of the unprocessed and glycoengineered SARS-CoV 2 spike protein
205 was achieved by the two orthogonal methods xCGE-LIF and MALDI-TOF-MS (see Figure 2
206 and Figure 3). The high-resolution *N*-glycan fingerprints (migration time aligned & and peak
207 height normalized electropherograms) from xCGE-LIF combined with the precise mass profiles
208 generated by MALDI-TOF-MS allowed for fast and robust annotation also of isomeric *N*-
209 glycan structures. Furthermore, normalization of *N*-glycan fingerprints to total peak height
210 enabled relative quantification of individual *N*-glycan structures by xCGE-LIF. The insect-cell-
211 produced recombinant SARS-CoV-2 spike glycoprotein prominently displays α -1,6-core-
212 fucosylated Man3F and G0F-Gn(3) structures (Figure 2A blue and Figure 3A). Moreover,
213 Man2F, Man3, the hybrid-type structure G0-Gn(3), the complex-type structure G0F, and
214 afucosylated oligomannose-type structures were detected. There is excellent agreement
215 between xCGE-LIF and MALDI-TOF-MS measurements.

216

217 **3.3 *In-vitro* glycoengineering of SARS-CoV-2 spike glycoprotein**

218 Recombinant MGAT1 Δ TM, MGAT2 Δ TM and GalT Δ TM were used in a one-pot
219 glycoengineering reaction to convert the paucimannose structures to complex-type *N*-glycans.
220 In scouting experiments it was found that after MGAT1 Δ TM, MGAT2 Δ TM and GalT Δ TM
221 addition at the start of the reaction, Man3F was converted to, at least in parts, to the hybrid-type
222 structure G1F-Gn(3) missing the extension on the α 1-6 mannosylated antenna catalysed by
223 MGAT2. G1F-Gn(3) is not a natural substrate for MGAT2 and can, if at all, most likely only
224 be processed at very low turnover rates. Thus, the reactions were carried out by adding the
225 enzymes sequentially as detailed in M&M. In the first step, a GlcNAc residue is added from
226 UDP-GlcNAc to the α -1,3-linked terminal mannose antenna of Man3F and Man3 by
227 MGAT1 Δ TM (see Figure 2A and Figure 3A and B). After a reaction time of 12 h only parts of
228 Man3 and Man3F were converted to G0-Gn(3) and G0F-Gn(3), respectively. Scouting
229 experiment showed that the conversion is typically irreversible and, thus, the incomplete
230 processing is either due to low turnover or possible enzyme inactivation of MGAT1 Δ TM.
231 Another possibility is that the glycans are inaccessible for MGAT1 Δ TM but can be released
232 from the backbone by PNGase F. In the second step, UDP-GlcNAc and MGAT2 Δ TM are added.
233 After incubation for 12 h, the hybrid-type structures G0-Gn(3) and G0F-Gn(3) were converted

234 to G0 and G0F, respectively, with only a minor fraction of G0F-Gn(3) remaining (Figure 2B
235 and Figure C). MGAT2 Δ TM did not show any activity towards Man3 and Man3F. However,
236 as mentioned before, this could be due the inaccessibility of these glycans. In the final step, the
237 reaction was supplemented with UDP-galactose and GalT Δ TM to add galactose to the terminal
238 GlcNAc. At the end point of the reaction, after another 12 h of incubation, the galactosylated
239 complex-type structure G2 was dominant along unprocessed Man3F (see Figure 2C and Figure
240 3D). Moreover, G0 was completely converted to G2 while the residual amount of the hybrid-
241 type structure G0F-Gn(3) was also galactosylated to G1F-Gn(3). All oligomannose-type
242 structures remained unaltered throughout the reaction. In general, the xCGE-LIF and the
243 MALDI-TOF-MS data were in excellent agreement for all measurements.

244

245

246 **4 Discussion**

247 Due to its scalability, eukaryotic protein processing and high productivity, the baculovirus-
248 insect cell expression system is well-suited for the production of subunit vaccines (Palomares
249 et al.;Felberbaum, 2015). In addition to subunit vaccines against SARS-CoV-2 infections in
250 development, there are currently three licensed vaccines, Flublok®, Cervarix® and Provenge®
251 produced using this expression system with several more in clinical trials (Palomares et
252 al.;Felberbaum, 2015).

253 High immunogenicity of a recombinant insect-cell produced spike protein ectodomain variant,
254 very similar to the one used here, has been confirmed in non-human primates [40]. Moreover,
255 the spike protein is the antigen target of virtually all COVID-19 vaccines and advanced vaccine
256 candidates (Krammer, 2020). At the time of writing this article, there was one licensed COVID-
257 19 protein subunit vaccine (RBD-Dimer from Anhui Zhifei Longcom Biopharmaceutical,
258 China) in China, while for two more candidates (Covovax from Novavax, USA; VAT00002
259 from Sanofi Pasteur and GSK, France / UK) emergency authorization was pending in the US
260 and Europe (Yang et al., 2020;Dai and Gao, 2021;Shrotri et al., 2021). All three are recombinant
261 SARS-CoV-2 spike protein variants produced using the baculovirus-insect cell expression
262 system (Kyriakidis et al., 2021).

263 Glycoforms of recombinant proteins produced using baculovirus-insect cell expression systems
264 are profoundly different from those produced using mammalian expression systems. An
265 extensive review on the glycosylation processing of insect cells is given by Geisler et al (Geisler
266 et al., 2015). Typically, these proteins display mainly paucimannose and hybrid-type *N*-glycans
267 with, at most, minor fractions of complex-type and oligomannose-type *N*-glycans (Palomares
268 et al.;Geisler et al., 2015). In this respect, the glycoform we observed on the pure spike protein
269 variants is exemplary for an insect cell protein expression.

270 For vaccine development, it has been proposed that immunogen candidates benefit from closely
271 mimicking the macro- and microheterogeneity of the live virus glycosylation (Grant et al.,
272 2020;Watanabe et al., 2020). This is as eliciting antibodies against shielded or non-native
273 epitopes could cause an inefficient immune response. To overcome such obstacles, novel
274 strategies utilizing distinct non-human glycans containing N-glycolylneuraminic acid or α ,1-3
275 linked galactose residues, have been proposed to alleviate immune responses (Schön et
276 al.;Hütter et al., 2013;Galili, 2020;Chen, 2021). However, such approaches still need to be
277 investigated in detail experimentally as, for example, both compounds are also suspected to
278 cause allergenic reactions in humans.

279 To convert the glycoform from primarily paucimannose-type to typical mammalian complex-
280 type *N*-glycans, the recombinant human glycosyltransferases, MGAT1 Δ TM, MGAT2 Δ TM and
281 GalT Δ TM, were effectively combined in a cell-free, one-pot glycosylation reaction. The gene
282 expression of these glycosyltransferases in *E. coli* and the activity of the His-tag purified,
283 soluble recombinant proteins in one-pot reactions using free glycans as substrates has been
284 shown before ((Fujiyama et al., 2001), Mahour *et al.*, unpublished).

285 The site-specific glycan analysis of recombinant SARS-CoV-2 spike protein ectodomain
286 expressed in human-derived cell line FreeStyleTM 293-F showed that of the 22 *N*-glycosylation
287 sites only eight contained substantial fractions of oligomannose-type *N*-glycans (Watanabe et
288 al., 2020). It is assumed that the occurrence of oligomannose-type fractions is caused by the
289 steric inaccessibility of these glycans to the glycan processing enzymes in the Golgi, i.e. the
290 occurrence of oligomannose-type *N*-glycans at distinct sites has shown to be independent of the
291 producer cell line for the HIV viral glycoprotein gp120 (Pritchard et al., 2015). In accordance
292 with the human cell-derived spike protein, our engineered spike protein abundantly exhibited
293 complex-type G2F *N*-glycans. To a minor extend, a range of hybrid- and oligomannose-type
294 *N*-glycans were also detected on the engineered spike protein. In contrast to the engineered
295 spike protein, human cell-derived spike proteins also exhibit complex-type multi-antennary and
296 sialylated structures (Watanabe et al., 2020). Taken together, a significant overlap of the
297 glycoform has been generated. Whether the overlap is also site-specific remains to be
298 investigated in future.

299 Over the past years, many efforts have been made to engineer insect cell lines to express
300 complex-type *N*-glycans. A comprehensive summary of the attempts is given by Palomares et
301 al. (Palomares et al.). Briefly, complex-type *N*-glycans can be produced by the co-expression
302 of glycosyltransferases or by generating transient insect cell lines. While the former generates
303 an additional metabolic burden and affects growth properties, the stability of the latter has not
304 been examined for commercial scale use. The advantage of *in-vitro* glycoengineering lies in its
305 independence of producer cell lines as well as its flexibility towards the option to readily
306 generate different glycoforms that are close to homogeneity. However, expensive nucleotides
307 sugars are required as substrates and, thus, it is so far not feasible to apply *in-vitro*
308 glycoengineering at larger scales (Mahour et al., 2018;Rexer et al., 2018;Rexer et al., 2020b).

309

310 **5. Conclusion**

311 SARS-CoV-2 spike glycoprotein variants produced in a baculovirus-insect cell expression
312 system were *in-vitro* glycoengineered using recombinant glycosyltransferases to mimic the
313 glycoform observed on the human cell-derived protein. *In-vitro* glycoengineering reactions as
314 conducted here, can be used to generate immunogen candidates for pre-clinical testing to
315 investigate the role of glycosylation on the antigenicity and immunogenicity in animal models.
316 In general, *in-vitro* glycoengineering approaches can virtually be used to tailor the glycoform
317 of all prominent vaccine candidates such as activated and attenuated viruses and virus like
318 particles. The application of the technology to larger scales depends on the bulk availability of
319 sugar nucleotides at moderate costs.

320

321 **6. Acknowledgement**

322 The project is funded by the Deutsche Forschungsgemeinschaft (DFG, German Research
323 Foundation) – Projektnummer 458633485. Dunja Bruder acknowledges funding from the State
324 of Saxony-Anhalt (Förderkenzeichen I 130). Erdmann Rapp und Valerian Grote acknowledge

325 funding by DFG- FOR2509: RA2992/1-1. Furthermore, the authors would like to thank Anja
326 Bastian for her excellent technical support. Lisa Wenzel and Reza Mahour are acknowledged
327 for help with the expression and purification of glycosyltransferases.

328
329

330 **7. Conflict of Interest**

331 ER and UR hold shares in glyXera GmbH. All other authors declare that the research was
332 conducted in the absence of any commercial or financial relationships that could be construed
333 as a potential conflict of interest.

334
335

336 **8. List of abbreviations**

APTS	8-Aminopyrene-1,3,6-trisulfonic acid
dH ₂ O	Deionized water
GlcNAc	<i>N</i> -acetylglucosamine
HEPES	4-(2-hydroxyethyl)-1-piperazineethanesulfonic acid
HILIC	Hydrophilic interaction liquid chromatography
His tag	Histidine tag
IMAC	Immobilized Metal Affinity Chromatography
IPTG	Isopropyl β -D-1-thiogalactopyranoside
LC	Liquid Chromatography
MALDI-TOF	Matrix-assisted laser desorption/ionization time-of-flight mass spectrometry
MS	Mass spectrometry
MnCl ₂	Mangan(II)-chlorid
MTU''	Migration Time Units after alignment to internal standards
rpm	Rounds per min
SDS-PAGE	Sodium dodecyl sulfate polyacrylamide gel electrophoresis
SPE	Solid-phase extraction
TPH	Total peak height
UDP-galactose	Uridine-diphosphate galactose
UDP-GlcNAc	Uridine diphosphate <i>N</i> -acetylglucosamine
xCGE-LIF	Multiplexed capillary gel electrophoresis with laser-induced fluorescence detection

337

338
339

340

341

342 **9 Literature**

- 343 Bagdonaite, I., and Wandall, H.H. (2018). Global aspects of viral glycosylation. *Glycobiology*
344 28, 443-467.
- 345 Behrens, A.-J., Vasiljevic, S., Pritchard, L.K., Harvey, D.J., Andev, R.S., Krumm, S.A.,
346 Struwe, W.B., Cupo, A., Kumar, A., Zitzmann, N., Seabright, G.E., Kramer, H.B.,
347 Spencer, D.I.R., Royle, L., Lee, J.H., Klasse, P.J., Burton, D.R., Wilson, I.A., Ward,
348 A.B., Sanders, R.W., Moore, J.P., Doores, K.J., and Crispin, M. (2016). Composition
349 and Antigenic Effects of Individual Glycan Sites of a Trimeric HIV-1 Envelope
350 Glycoprotein. *Cell Reports* 14, 2695-2706.
- 351 Bendiak, B. (2014). "Mannosyl (Alpha-1,6-)-Glycoprotein Beta-1,2-N-
352 Acetylglucosaminyltransferase (MGAT2)," in *Handbook of Glycosyltransferases and*
353 *Related Genes*, eds. N. Taniguchi, K. Honke, M. Fukuda, H. Narimatsu, Y.
354 Yamaguchi & T. Angata. (Tokyo: Springer Japan), 195-207.
- 355 Boeggeman, E.E., Ramakrishnan, B., and Qasba, P.K. (2003). The N-terminal stem region of
356 bovine and human β 1,4-galactosyltransferase I increases the in vitro folding efficiency
357 of their catalytic domain from inclusion bodies. *Protein Expression and Purification*
358 30, 219-229.
- 359 Chen, J.-M. (2021). SARS-CoV-2 replicating in nonprimate mammalian cells probably have
360 critical advantages for COVID-19 vaccines due to anti-Gal antibodies: A minireview
361 and proposals. *Journal of Medical Virology* 93, 351-356.
- 362 Chen, W.-H., Du, L., Chag, S.M., Ma, C., Tricoche, N., Tao, X., Seid, C.A., Hudspeth, E.M.,
363 Lustigman, S., Tseng, C.-T.K., Bottazzi, M.E., Hotez, P.J., Zhan, B., and Jiang, S.
364 (2014). Yeast-expressed recombinant protein of the receptor-binding domain in
365 SARS-CoV spike protein with deglycosylated forms as a SARS vaccine candidate.
366 *Human Vaccines & Immunotherapeutics* 10, 648-658.
- 367 Cymer, F., Beck, H., Rohde, A., and Reusch, D. (2018). Therapeutic monoclonal antibody N-
368 glycosylation – Structure, function and therapeutic potential. *Biologicals* 52, 1-11.
- 369 Dai, L., and Gao, G.F. (2021). Viral targets for vaccines against COVID-19. *Nature reviews.*
370 *Immunology* 21, 73-82.
- 371 Dalziel, M., Crispin, M., Scanlan, C.N., Zitzmann, N., and Dwek, R.A. (2014). Emerging
372 Principles for the Therapeutic Exploitation of Glycosylation. *Science* 343, 1235681-
373 1235681 - 1235681-1235688.
- 374 Felberbaum, R.S. (2015). The baculovirus expression vector system: A commercial
375 manufacturing platform for viral vaccines and gene therapy vectors. *Biotechnology*
376 *Journal* 10, 702-714.
- 377 Fischöder, T., Cajic, S., Grote, V., Heinzler, R., Reichl, U., Franzreb, M., Rapp, E., and
378 Elling, L. 2019. Enzymatic Cascades for Tailored $^{13}\text{C}_6$ and ^{15}N Enriched Human Milk
379 Oligosaccharides. *Molecules* [Online], 24. Available: [https://www.mdpi.com/1420-](https://www.mdpi.com/1420-3049/24/19/3482)
380 [3049/24/19/3482](https://www.mdpi.com/1420-3049/24/19/3482).
- 381 Francica, J.R., Varela-Rohena, A., Medvec, A., Plesa, G., Riley, J.L., and Bates, P. 2010.
382 Steric shielding of surface epitopes and impaired immune recognition induced by the
383 ebola virus glycoprotein. *PLoS Pathog* [Online], 6. [Accessed Sep 9].
- 384 Fujiyama, K., Ido, Y., Misaki, R., Moran, D.G., Yanagihara, I., Honda, T., Nishimura, S.I.,
385 Yoshida, T., and Seki, T. (2001). Human N-Acetylglucosaminyltransferase I.
386 Expression in *Escherichia coli* as a soluble enzyme, and application as an immobilized
387 enzyme for the chemoenzymatic synthesis of N-linked oligosaccharides. *Journal of*
388 *Bioscience and Bioengineering* 92, 569-574.
- 389 Galili, U. (2020). Amplifying immunogenicity of prospective Covid-19 vaccines by
390 glycoengineering the coronavirus glycan-shield to present α -gal epitopes. *Vaccine* 38,
391 6487-6499.

- 392 Geisler, C., Mabashi-Asazuma, H., and Jarvis, D.L. (2015). "An overview and history of
393 glyco-engineering in insect expression systems," in *Glyco-Engineering: Methods and*
394 *Protocols.*), 131-152.
- 395 Go, E.P., Ding, H., Zhang, S., Ringe, R.P., Nicely, N., Hua, D., Steinbock, R.T., Golabek, M.,
396 Alin, J., Alam, S.M., Cupo, A., Haynes, B.F., Kappes, J.C., Moore, J.P., Sodroski,
397 J.G., and Desaire, H. 2017. Glycosylation Benchmark Profile for HIV-1 Envelope
398 Glycoprotein Production Based on Eleven Env Trimers. *Journal of Virology* [Online],
399 91. Available: <https://jvi.asm.org/content/jvi/91/9/e02428-16.full.pdf>.
- 400 Gram, A.M., Oosenbrug, T., Lindenbergh, M.F.S., Bull, C., Comvalius, A., Dickson, K.J.I.,
401 Wiegant, J., Vrolijk, H., Lebbink, R.J., Wolterbeek, R., Adema, G.J., Griffioen, M.,
402 Heemskerck, M.H.M., Tschärke, D.C., Hutt-Fletcher, L.M., Wiertz, E.J.H.J., Hoeben,
403 R.C., and Rensing, M.E. (2016). The Epstein-Barr Virus Glycoprotein gp150 Forms an
404 Immune-Evasive Glycan Shield at the Surface of Infected Cells. *Plos Pathogens* 12.
- 405 Grant, O.C., Montgomery, D., Ito, K., and Woods, R.J. 2020. Analysis of the SARS-CoV-2
406 spike protein glycan shield reveals implications for immune recognition. *Scientific*
407 *Reports* [Online], 10. Available: <https://doi.org/10.1038/s41598-020-71748-7>
408 [Accessed 2020/09/14].
- 409 Helle, F., Duverlie, G., and Dubuisson, J. (2011). The Hepatitis C Virus Glycan Shield and
410 Evasion of the Humoral Immune Response. *Viruses-Basel* 3, 1909-1932.
- 411 Hennig, R., Cajic, S., Borowiak, M., Hoffmann, M., Kottler, R., Reichl, U., and Rapp, E.
412 (2016). Towards personalized diagnostics via longitudinal study of the human plasma
413 N-glycome. *Biochimica et Biophysica Acta (BBA) - General Subjects* 1860, 1728 -
414 1738.
- 415 Hennig, R., Rapp, E., Kottler, R., Cajic, S., Borowiak, M., and Reichl, U. (2015). "N-
416 Glycosylation fingerprinting of viral glycoproteins by xCGE-LIF", in: *Methods in*
417 *Molecular Biology*. Humana Press Inc.).
- 418 Hütter, J., Rödig, J.V., Höper, D., Seeberger, P.H., Reichl, U., Rapp, E., and Lepenies, B.
419 (2013). Toward Animal Cell Culture-based Influenza Vaccine Design: Viral
420 Hemagglutinin N-Glycosylation Markedly Impacts Immunogenicity. *The Journal of*
421 *Immunology* 190, 220 - 230.
- 422 Imperiali, B., and O'connor, S.E. (1999). Effect of N-linked glycosylation on glycopeptide
423 and glycoprotein structure. *Current Opinion in Chemical Biology* 3, 643-649.
- 424 Krammer, F. (2020). SARS-CoV-2 vaccines in development. *Nature* 586, 516-527.
- 425 Kyriakidis, N.C., López-Cortés, A., González, E.V., Grimaldos, A.B., and Prado, E.O. 2021.
426 SARS-CoV-2 vaccines strategies: a comprehensive review of phase 3 candidates. *npj*
427 *Vaccines* [Online], 6. Available: <https://doi.org/10.1038/s41541-021-00292-w>
428 [Accessed 2021/02/22].
- 429 Li, D., Von Schaewen, M., Wang, X., Tao, W., Zhang, Y., Li, L., Heller, B., Hrebikova, G.,
430 Deng, Q., Ploss, A., Zhong, J., and Huang, Z. (2016). Altered Glycosylation Patterns
431 Increase Immunogenicity of a Subunit Hepatitis C Virus Vaccine, Inducing
432 Neutralizing Antibodies Which Confer Protection in Mice. *Journal of Virology* 90,
433 10486-10498.
- 434 Lin, G., Simmons, G., Pöhlmann, S., Baribaud, F., Ni, H., Leslie, G.J., Haggarty, B.S., Bates,
435 P., Weissman, D., Hoxie, J.A., and Doms, R.W. (2003). Differential N-Linked
436 Glycosylation of Human Immunodeficiency Virus and Ebola Virus Envelope
437 Glycoproteins Modulates Interactions with DC-SIGN and DC-SIGNR. *Journal of*
438 *Virology* 77, 1337-1346.
- 439 Lin, S.-C., Jan, J.-T., Dionne, B., Butler, M., Huang, M.-H., Wu, C.-Y., Wong, C.-H., and
440 Wu, S.-C. 2013. Different Immunity Elicited by Recombinant H5N1 Hemagglutinin
441 Proteins Containing Pauci-Mannose, High-Mannose, or Complex Type N-Glycans.
442 *PLOS ONE* [Online], 8. Available: <https://doi.org/10.1371/journal.pone.0066719>.

- 443 Mahour, R., Klapproth, J., Rexer, T.F.T., Schildbach, A., Klamt, S., Pietzsch, M., Rapp, E.,
444 and Reichl, U. (2018). Establishment of a five-enzyme cell-free cascade for the
445 synthesis of uridine diphosphate N-acetylglucosamine. *Journal of Biotechnology* 283,
446 120-129.
- 447 Neelamegham, S., Aoki-Kinoshita, K., Bolton, E., Frank, M., Lisacek, F., Lütteke, T.,
448 O'boyle, N., Packer, N.H., Stanley, P., Toukach, P., Varki, A., Woods, R.J., and
449 Group, T.S.D. (2019). Updates to the Symbol Nomenclature for Glycans guidelines.
450 *Glycobiology* 29, 620-624.
- 451 Palomares, L.A., Srivastava, I.K., Ramírez, O.T., and Cox, M.M.J. "Glycobiotechnology of
452 the Insect Cell-Baculovirus Expression System Technology." (Berlin, Heidelberg:
453 Springer Berlin Heidelberg), 1-22.
- 454 Pralow, A., Hoffmann, M., Nguyen-Khuong, T., Pioch, M., Hennig, R., Genzel, Y., Rapp, E.,
455 and Reichl, U. Comprehensive N-glycosylation analysis of the influenza A virus
456 proteins HA and NA from adherent and suspension MDCK cells. *The FEBS Journal*.
- 457 Pritchard, L.K., Harvey, D.J., Bonomelli, C., Crispin, M., and Doores, K.J. (2015). Cell- and
458 Protein-Directed Glycosylation of Native Cleaved HIV-1 Envelope. *Journal of*
459 *Virology* 89, 8932-8944.
- 460 Ramakrishnan, B., and Qasba, P.K. (2014). "UDP-Gal: BetaGlcNAc Beta 1,4-
461 Galactosyltransferase, Polypeptide 1 (B4GALT1)," in *Handbook of*
462 *Glycosyltransferases and Related Genes*, eds. N. Taniguchi, K. Honke, M. Fukuda, H.
463 Narimatsu, Y. Yamaguchi & T. Angata. (Tokyo: Springer Japan), 51-62.
- 464 Rexer, T.F.T., Laaf, D., Gottschalk, J., Frohnmeyer, J., Rapp, E., and Elling, L. (2020a).
465 "Enzymatic synthesis of glycans and glycoconjugates," in *Advances in*
466 *Glycobiotechnology*, eds. E. Rapp & U. Reichl. Springer Nature).
- 467 Rexer, T.F.T., Schildbach, A., Klapproth, J., Schierhorn, A., Mahour, R., Pietzsch, M., Rapp,
468 E., and Reichl, U. (2018). One pot synthesis of GDP-mannose by a multi-enzyme
469 cascade for enzymatic assembly of lipid-linked oligosaccharides. *Biotechnology and*
470 *Bioengineering* 115, 192-205.
- 471 Rexer, T.F.T., Wenzel, L., Hoffmann, M., Tischlik, S., Bergmann, C., Grote, V., Boecker, S.,
472 Bettenbrock, K., Schildbach, A., Kottler, R., Mahour, R., Rapp, E., Pietzsch, M., and
473 Reichl, U. (2020b). Synthesis of lipid-linked oligosaccharides by a compartmentalized
474 multi-enzyme cascade for the in vitro N-glycosylation of peptides. *Journal of*
475 *Biotechnology* 322, 54-65.
- 476 Rödig, J., Rapp, E., Djeljadini, S., Lohr, V., Genzel, Y., Jordan, I., Sandig, V., and Reichl, U.
477 (2011). Impact of Influenza Virus Adaptation Status on HA N-Glycosylation Patterns
478 in Cell Culture-Based Vaccine Production. *Journal of Carbohydrate Chemistry* 30,
479 281 - 290.
- 480 Rödig, J.V., Rapp, E., Bohne, J., Kampe, M., Kaffka, H., Bock, A., Genzel, Y., and Reichl, U.
481 (2013). Impact of cultivation conditions on N-glycosylation of influenza virus a
482 hemagglutinin produced in MDCK cell culture. *Biotechnology and Bioengineering*
483 110, 1691-1703.
- 484 Schön, K., Lepenies, B., and Goyette-Desjardins, G. "Impact of Protein Glycosylation on the
485 Design of Viral Vaccines." (Berlin, Heidelberg: Springer Berlin Heidelberg), 1-36.
- 486 Schwarzer, J., Rapp, E., Hennig, R., Genzel, Y., Jordan, I., Sandig, V., and Reichl, U. (2009).
487 Glycan analysis in cell culture-based influenza vaccine production: Influence of host
488 cell line and virus strain on the glycosylation pattern of viral hemagglutinin. *Vaccine*
489 27, 4325-4336.
- 490 Selman, M.H.J., Hemayatkar, M., Deelder, A.M., and Wuhrer, M. (2011). Cotton HILIC SPE
491 Microtips for Microscale Purification and Enrichment of Glycans and Glycopeptides.
492 *Analytical Chemistry* 83, 2492-2499.

- 493 Shrotri, M., Swinnen, T., Kampmann, B., and Parker, E.P.K. (2021). An interactive website
494 tracking COVID-19 vaccine development. *Lancet Glob Health*.
- 495 Sommerstein, R., Flatz, L., Remy, M.M., Malinge, P., Magistrelli, G., Fischer, N., Sahin, M.,
496 Bergthaler, A., Igonet, S., Ter Meulen, J., Rigo, D., Meda, P., Rabah, N., Coutard, B.,
497 Bowden, T.A., Lambert, P.-H., Siegrist, C.-A., and Pinschewer, D.D. (2015).
498 Arenavirus Glycan Shield Promotes Neutralizing Antibody Evasion and Protracted
499 Infection. *Plos Pathogens* 11.
- 500 Stanley, P. (2014). "Mannosyl (alpha-1,3-)-glycoprotein beta-1,2-
501 NAcetylglucosaminyltransferase (MGAT1)," in *Handbook of Glycosyltransferases
502 and Related Genes, Second Edition.*, 183-194.
- 503 Stanley, P., Taniguchi, N., and Aebi, M. (2015). "N-Glycans," in *Essentials of Glycobiology*,
504 eds. A. Varki, R.D. Cummings, J.D. Esko, P. Stanley, G.W. Hart, M. Aebi, A.G.
505 Darvill, T. Kinoshita, N.H. Packer, J.H. Prestegard, R.L. Schnaar & P.H. Seeberger.
506 (Cold Spring Harbor (NY): Cold Spring Harbor Laboratory Press), 99-111.
- 507 Tsuchiya, S., Aoki, N.P., Shinmachi, D., Matsubara, M., Yamada, I., Aoki-Kinoshita, K.F.,
508 and Narimatsu, H. (2017). Implementation of GlycanBuilder to draw a wide variety of
509 ambiguous glycans. *Carbohydrate Research* 445, 104-116.
- 510 Van Landuyt, L., Lonigro, C., Meuris, L., and Callewaert, N. (2019). Customized protein
511 glycosylation to improve biopharmaceutical function and targeting. *Current Opinion
512 in Biotechnology* 60, 17-28.
- 513 Varki, A. (2017). Biological roles of glycans. *Glycobiology* 27, 3-49.
- 514 Walls, A.C., Park, Y.-J., Tortorici, M.A., Wall, A., McGuire, A.T., and Velesler, D. (2020).
515 Structure, Function, and Antigenicity of the SARS-CoV-2 Spike Glycoprotein. *Cell*
516 181, 281-292.
- 517 Walls, A.C., Tortorici, M.A., Frenz, B., Snijder, J., Li, W., Rey, F.A., Dimairo, F., Bosch, B.-
518 J., and Velesler, D. (2016). Glycan shield and epitope masking of a coronavirus spike
519 protein observed by cryo-electron microscopy. *Nature Structural & Molecular
520 Biology* 23, 899-905.
- 521 Wan, Y., Shang, J., Graham, R., Baric, R.S., and Li, F. 2020. Receptor Recognition by the
522 Novel Coronavirus from Wuhan: an Analysis Based on Decade-Long Structural
523 Studies of SARS Coronavirus. *Journal of Virology* [Online], 94. Available:
524 <https://jvi.asm.org/content/jvi/94/7/e00127-20.full.pdf>.
- 525 Watanabe, Y., Allen, J.D., Wrapp, D., McLellan, J.S., and Crispin, M. (2020). Site-specific
526 glycan analysis of the SARS-CoV-2 spike. *Science* 369, 330-333.
- 527 Watanabe, Y., Bowden, T.A., Wilson, I.A., and Crispin, M. (2019). Exploitation of
528 glycosylation in enveloped virus pathobiology. *Biochimica et Biophysica Acta (BBA) -
529 General Subjects* 1863, 1480-1497.
- 530 Wrapp, D., Wang, N., Corbett, K.S., Goldsmith, J.A., Hsieh, C.L., Abiona, O., Graham, B.S.,
531 and McLellan, J.S. (2020). Cryo-EM structure of the 2019-nCoV spike in the prefusion
532 conformation. *Science* 367, 1260-1263.
- 533 Yang, J., Wang, W., Chen, Z., Lu, S., Yang, F., Bi, Z., Bao, L., Mo, F., Li, X., Huang, Y.,
534 Hong, W., Yang, Y., Zhao, Y., Ye, F., Lin, S., Deng, W., Chen, H., Lei, H., Zhang, Z.,
535 Luo, M., Gao, H., Zheng, Y., Gong, Y., Jiang, X., Xu, Y., Lv, Q., Li, D., Wang, M.,
536 Li, F., Wang, S., Wang, G., Yu, P., Qu, Y., Yang, L., Deng, H., Tong, A., Li, J.,
537 Wang, Z., Yang, J., Shen, G., Zhao, Z., Li, Y., Luo, J., Liu, H., Yu, W., Yang, M., Xu,
538 J., Wang, J., Li, H., Wang, H., Kuang, D., Lin, P., Hu, Z., Guo, W., Cheng, W., He,
539 Y., Song, X., Chen, C., Xue, Z., Yao, S., Chen, L., Ma, X., Chen, S., Gou, M., Huang,
540 W., Wang, Y., Fan, C., Tian, Z., Shi, M., Wang, F.-S., Dai, L., Wu, M., Li, G., Wang,
541 G., Peng, Y., Qian, Z., Huang, C., Lau, J.Y.-N., Yang, Z., Wei, Y., Cen, X., Peng, X.,
542 Qin, C., Zhang, K., Lu, G., and Wei, X. (2020). A vaccine targeting the RBD of the S
543 protein of SARS-CoV-2 induces protective immunity. *Nature* 586, 572-577.

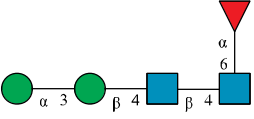
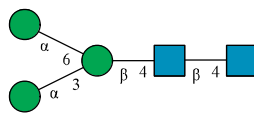
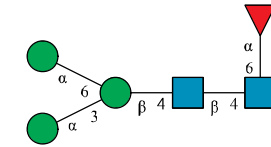
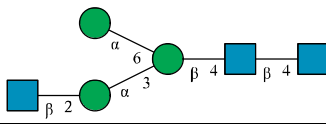
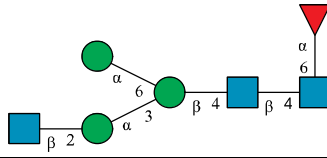
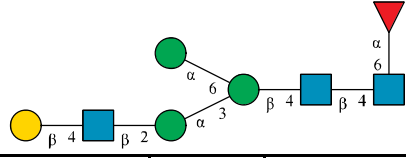
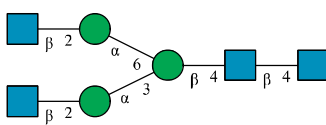
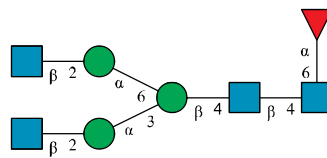
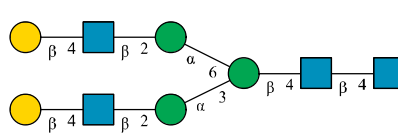
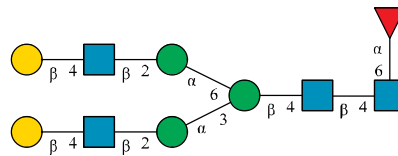
544 Zhou, P., Yang, X.-L., Wang, X.-G., Hu, B., Zhang, L., Zhang, W., Si, H.-R., Zhu, Y., Li, B.,
545 Huang, C.-L., Chen, H.-D., Chen, J., Luo, Y., Guo, H., Jiang, R.-D., Liu, M.-Q., Chen,
546 Y., Shen, X.-R., Wang, X., Zheng, X.-S., Zhao, K., Chen, Q.-J., Deng, F., Liu, L.-L.,
547 Yan, B., Zhan, F.-X., Wang, Y.-Y., Xiao, G.-F., and Shi, Z.-L. (2020). A pneumonia
548 outbreak associated with a new coronavirus of probable bat origin. *Nature* 579, 270-
549 273.

550

551

552 **List of Tables**

553 **Table 1.** *N*-glycan categories and nomenclature for all detected and referenced structures with
 554 the exception of oligomannose-type *N*-glycans. The monosaccharide building blocks are
 555 mannose (green circle), GlcNAc (blue square), fucose (red triangle) and galactose (yellow
 556 circle).

Paucimannose-type	Mans2F			
	Man3		Man3F	
Hybrid-type	G0-Gn(3)		G0F-Gn(3)	
	G1F-Gn(3)			
Complex-type	G0		G0F	
	G2		G2F	

557

558

559 **List of Figures**
560

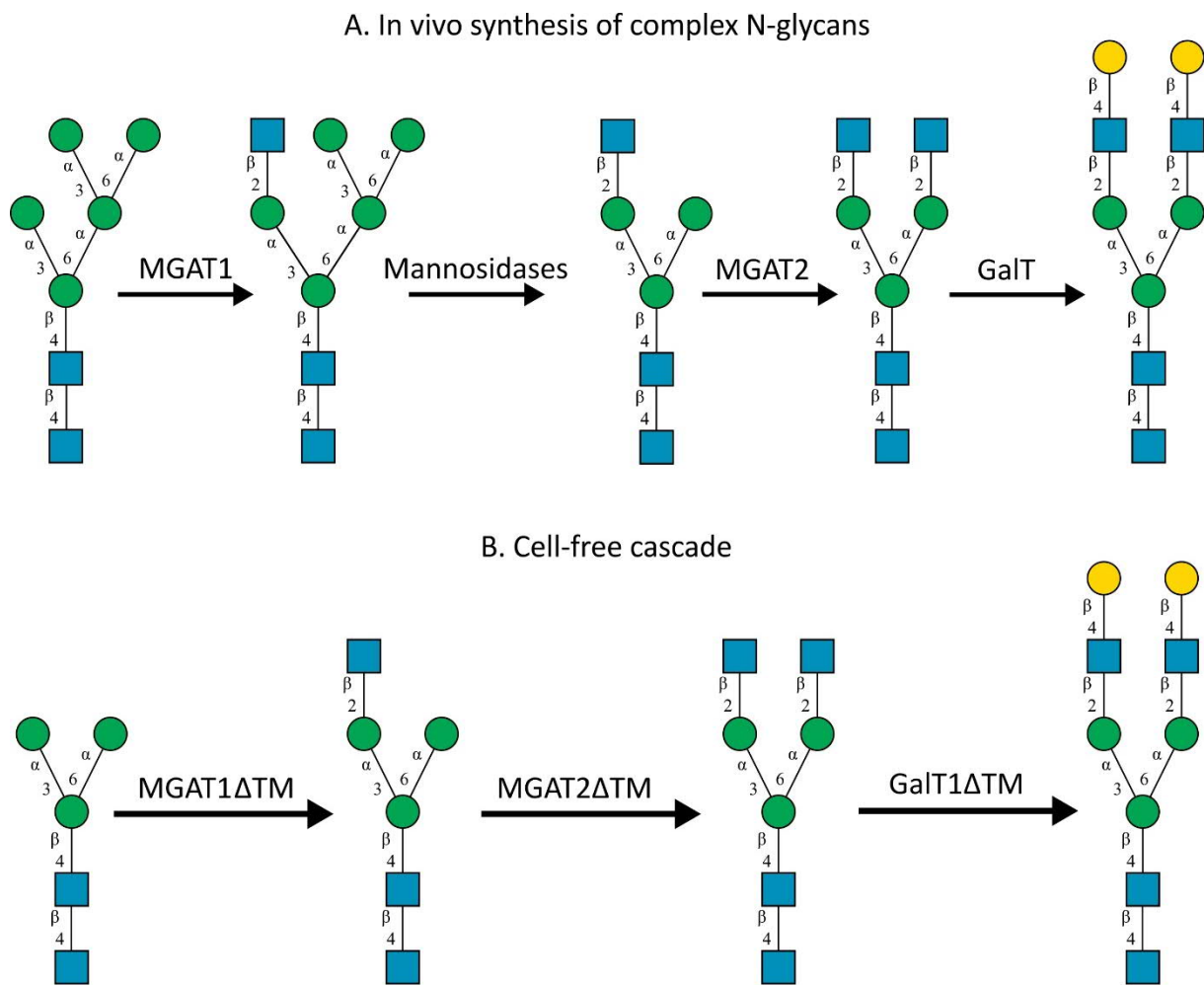
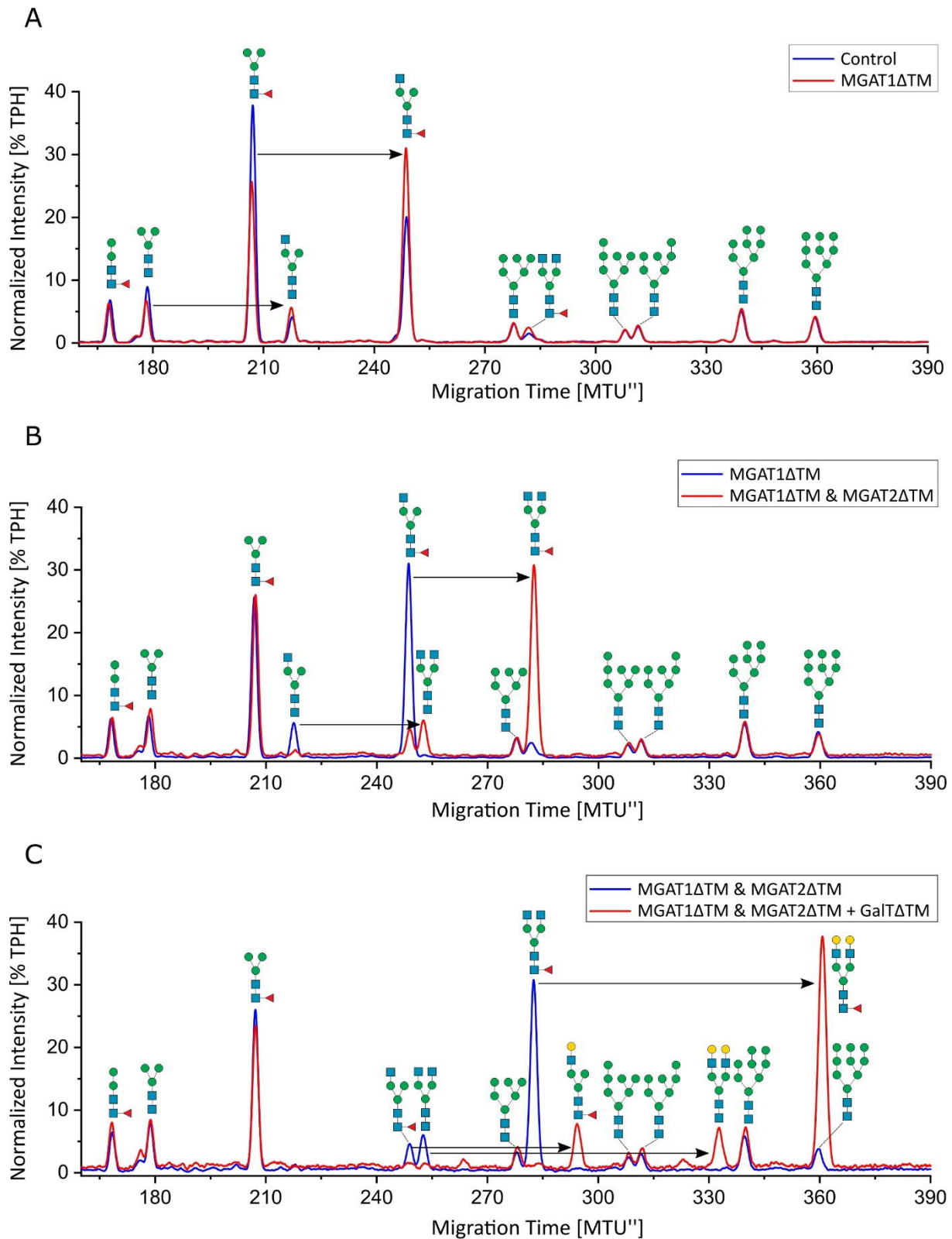
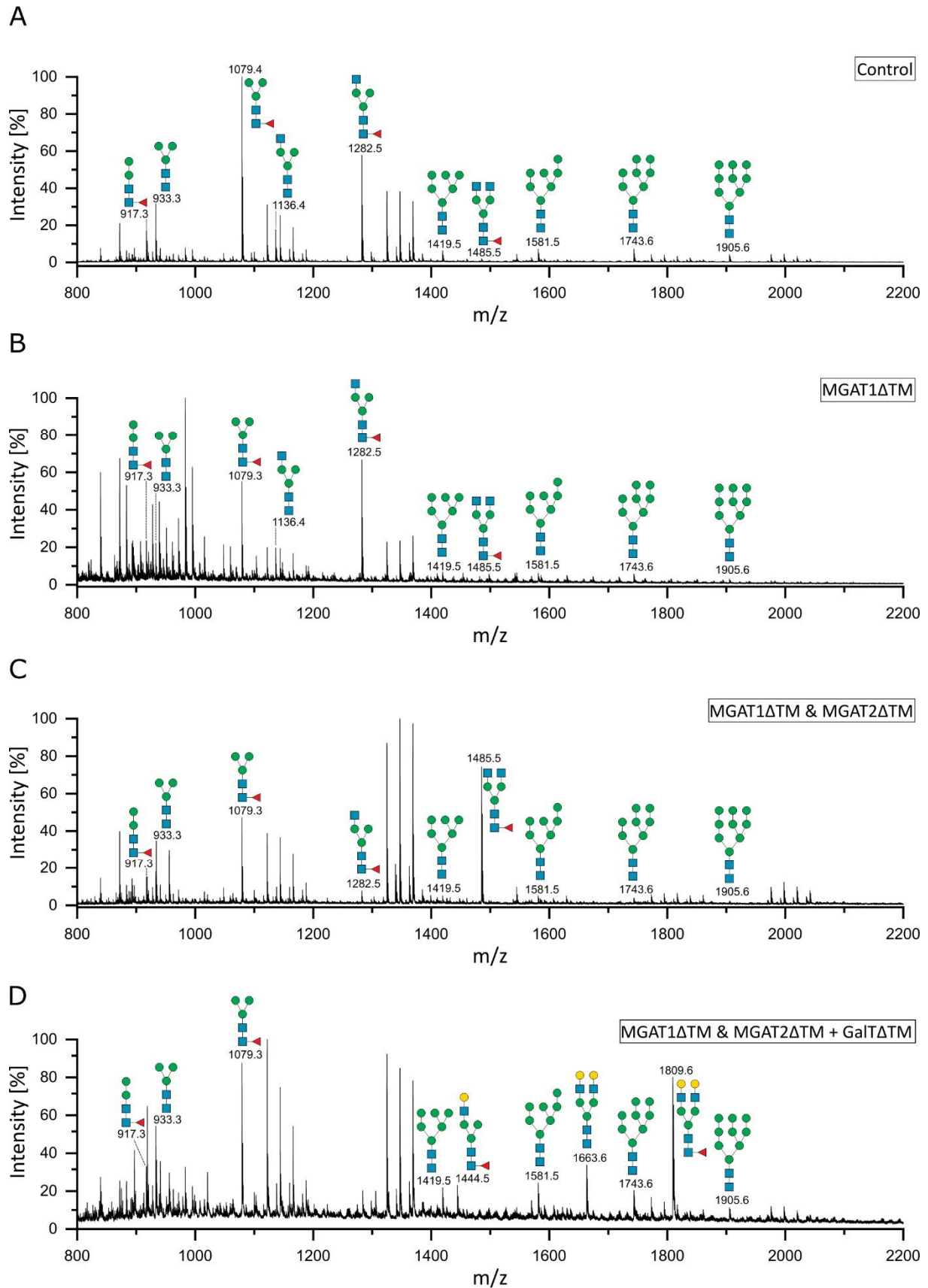


Figure 1. A) *In-vivo* the oligomannose-type N-glycan Man5 is converted into complex-type N-glycans by mannosidases and MGAT1, MGAT2 and GalT. Substrates for these reactions are UDP-GlcNAc and UDP-galactose, respectively. B) This process can be remodelled *in-vitro* to synthesize complex-type structures on insect cell-derived recombinant proteins with paucimannose-type N-glycans, like Man3.



569
570
571
572
573
574
575
576
577

Figure 2. xCGE-LIF *N*-glycan fingerprints of unprocessed and *in-vitro* glycoengineered SARS-CoV-2 spike protein *N*-glycans. *N*-glycosylation pattern of the spike protein: A) unprocessed (blue) and 12 h after start of the reaction with MGAT1ΔTM (red); B) 12 h after start of the reaction with MGAT1ΔTM (blue) and 12 h after the addition of MGAT2ΔTM (red); C) 12 h after the addition of MGAT2ΔTM (blue) and 12 h after addition of GalTΔTM (red). TPH, total peak height.



578
579

580 **Figure 3.** MALDI-TOF mass spectra of the unprocessed and glycoengineered SARS-CoV 2
581 spike protein glycoforms. *N*-glycans were detected in reflectron positive ion mode as sodium
582 adducts ($[M+Na]^+$). A) Unprocessed spike protein. B.) 12 h after start of the reaction with

583 MGAT1 Δ TM. C) 12 h after the addition of MGAT2 Δ TM. D) 12 h after the addition of
584 GalT Δ TM. Only the peaks that depict *N*-glycans are annotated.